Catalysis Today

Review

In-situ synthesis of hydrogen peroxide in tandem with selective oxidation reactions: A mini-review

B. Puértolas [a], A.K. Hill [b], T. García [a],*, B. Solsona [c],**, Laura Torrente-Murciano [b],***

[a] *Instituto de Carboquímica (ICB-CSIC), 50018 Zaragoza, Spain*
[b] *Department of Chemical Engineering, University of Bath, UK*
[c] *Department d'Enginyeria Química, Universitat de Valencia, Valencia, Spain*

A B S T R A C T

One-pot combination of the *in-situ* generation of hydrogen peroxide (H_2O_2) with selective oxidation reactions enhances the environmental and economic attractiveness of the use of H_2O_2 as green oxidant at industrial scale. This tandem reaction improves not only the safety aspects associated to H_2O_2 storage and transportation but also reduces the capital and operation costs. This review covers the progress in the field focussing on the areas of catalysis development, mechanistic understanding and engineering approaches (such as membrane reactors) for specific systems involving epoxidation of propylene oxide, hydroxylation of benzene, oxygenate synthesis from methane and Fenton processes, highlighting the main challenges to overcome in the near future.

Contents

1. Introduction

Hydrogen peroxide (H_2O_2) is currently presented as an attractive alternative to the industrial use of oxidants such as tBuOOH, N_2O, NaClO, chromate or permanganate [1,2]. These stoichiometric oxidants produce large amounts of waste by-products requiring additional purification and separation steps. In contrast, hydrogen peroxide is a highly active and selective oxidation agent for many

* Corresponding author. Tel.: +34 976 733977.
** Corresponding author. Tel.: +34 96 35 43735.
*** Corresponding author. Tel: +44 125 385857.
    E-mail addresses: tomas@icb.csic.es (T. García), benjamin.solsona@uv.es
(B. Solsona), ltm20@bath.ac.uk (L. Torrente-Murciano).

oxidation reactions with a high active oxygen content (47 wt%) producing only water as a co-product [3]. Additionally, hydrogen peroxide normally presents a higher oxidation potential than molecular oxygen, being efficient in a wide range of reaction conditions both acidic and basic. An important breakthrough in this field took place in 2008 with the commercialisation of the epoxidation of propylene with H_2O_2 to obtain propylene oxide (HPPO process) using titanium silicalite (TS-1) as a catalyst. Currently there are two HPPO-process plants jointly developed by BASF and Dow in Belgium and Thailand which finished their start-up in 2008 and 2011, respectively [4,5].

Currently, hydrogen peroxide is industrially produced *via* the anthraquinone route. Simplistically, in this process, an alkyl anthraquinone is used as a carrier which is firstly hydrogenated and later oxidised, releasing hydrogen peroxide [3]. One of the main advantages of this system is its capability of producing highly concentrated H_2O_2 which is normally marketed with concentrations ranging from 35 to 50 wt% or even above, however, the transportation and storage of H_2O_2 in concentrated form presents associated safety and economic issues. Currently, there is great scientific and industrial interest in the direct synthesis of hydrogen peroxide from molecular hydrogen and oxygen as a way of resolving its current challenges and potentially reducing its price [6,7]. Additionally, despite the relatively low concentration of H_2O_2 achieved during its direct synthesis compared to the high concentration solutions *via* the anthraquinone route, it aligns with the requirement for oxidation reactions (3–5 wt%).

Most of the current research in the area of direct synthesis of H_2O_2 as an oxidising agent focuses on the development of highly active and selective noble metal catalysts, with emphasis on gold and gold-palladium due their high yield stability [6,8,9]. Despite recent progress in the area [7], its large-scale application is mainly limited by its parallel decomposition into H_2 and water on the metal surface, decreasing the hydrogen efficiency of the process compromising its economic feasibility. Different strategies are currently being explored to overcome this problem [6], being the one-pot direct synthesis and utilisation of H_2O_2 one of the most elegant approaches [10–12]. In this way, *in-situ* generated hydrogen peroxide from molecular oxygen and hydrogen is simultaneously used for oxidation without the requirement of intermediate purification and/or separation steps. This integration of processes presents obvious advantages towards the reduction of the capital and operational costs which are expected to further the enhancement of the economic attractiveness of the use of hydrogen peroxide at industrial scale. Further safety benefits are gained by the lack of transportation and storage of hydrogen peroxide. Additionally, a controlled feeding of the desired concentrations of hydrogen peroxide in the system can be naturally achieved and tuned depending on the oxidation requirements. Considering these advantages, it is not surprising that the study of oxidation reactions using *in-situ* generated hydrogen peroxide has always been of great scientific interest, especially within the green chemistry movement. Consequently, the number of articles devoted to this tandem reaction has exponentially increased since the first studies in the 90s with most of the early progress covered in a review article by Clerici et al. in the late 90s [10]. Since then, significant progress has taken place in the areas of catalyst development, mechanistic understanding and engineering approaches such as the application of membrane reactors which are reviewed here. Focus has been directed towards specific systems involving epoxidation of propylene oxide, the hydroxylation of benzene, oxygenate synthesis from methane and Fenton processes due to their industrial potential. This review also highlights some of the current limitations in this tandem system that must be considered for future developments such the lower overall yields to oxidation products

compared to the use of pre-synthesised hydrogen peroxide, the high flammability of H_2/O_2 mixtures and H_2 efficiency.

2. Propylene epoxidation to propylene oxide

The selective oxidation of hydrocarbons is one of the most important processes for producing oxygenates, which are used as key intermediates in organic synthesis. One example of a high value oxygenate is propylene oxide (hereafter denoted as PO) which is mainly used as a feedstock for producing urethane polyols and propylene glycol.

The selective oxidation of propylene with molecular oxygen has been demonstrated to be very difficult to carry out as low yields and selectivity to PO are obtained. Thus, most of the industrial processes for PO production use clorohydrin or hydroperoxides in a two-stage process, which involves additional separation and/or purification units that increase the overall cost of the process. Recently a new process called hydrogen peroxide to propylene oxide (HPPO process) based on the selective oxidation of propylene with hydrogen peroxide has been implemented in Belgium and Thailand [4,5]. The HPPO process presents significant advantages from an economical and environmental point of view over former systems based on clorohydrin or tert-butyl peroxide such as the lower purification costs, the decrease in wastewater and the required energy input.

An interesting alternative to the HPPO process is the synthesis of PO by selective oxidation with *in-situ* generated H_2O_2 from oxygen and hydrogen, which can be undertaken in both liquid or vapour phase. Most of the studies in this area involve the use of metal nanoparticles supported on titanium-based materials as catalytic systems. Gold attracts most of the attention, however, there are also studies based on silver or other precious metals such as platinum or palladium. It is generally agreed that the role of the metallic species is mainly to produce hydrogen peroxide from H_2 and O_2 which is then converted into hydroperoxide-like species at the Ti sites of the support [8,13–28]. However, the metallic species can also be involved in the epoxidation reaction itself. An IR spectroscopic study [29] showed that the presence of gold nanoparticles on titania also catalyses the reaction between propylene and titania sites forming a bidentate propoxy species, similar to that formed by prolylene adsorbed on titania. The gold nanoparticles also catalysed the consecutive oxidation of the bidentate species to form carbonate/carboxylate species, which could be the cause of catalyst deactivation as discussed below. In the presence of H_2 and O_2, the intermediate bidentate propoxy species can desorb from the catalyst surface forming peroxide species over gold as the rate determining step [22,29,30]. Therefore, the mechanism of epoxidation of propylene over metallic-based catalysts can be simplistically described by the following steps [31,32]: (i) Propylene adsorbs on the titania-based support to produce bidentate propoxy species. (ii) Simultaneously, hydrogen and oxygen produce hydroperoxide-like species (OOH or H_2O_2) on the metallic surface and (iii) The peroxide species aid the desorption of the bidentate propoxy species from the catalyst, producing propylene oxide and water and restoring the support to its original state. Alternatively, these bidentate propoxy species could be further oxidised to produce strongly adsorbed carboxylate species causing the loss of the activity of the catalyst. Despite the synergetic role of the support and the metal nanoparticles in the tandem reaction, the effect of both is going to be considered separately for the sake of structure and clarity, however, one should consider both simultaneously when designing selective and active catalytic systems.

2.1. The effect of the support

The catalytic support has two main roles in the tandem *in-situ* generated H_2O_2 and epoxidation of propylene. It contains the titanium active sites for the adsorption of propylene and its further epoxidation and it is responsible of the dispersion of the metal species. Additionally, depending on its structure, the support can also play a role in the catalyst deactivation. The presence of Ti sites in tetrahedral-coordination is crucial for catalytic activity in detriment to those Ti sites in octahedral coordination. Tetrahedral coordinated Ti sites are found not only to be favourable for attaining small gold nanoparticles and consequently a high metal dispersion [33] but also to be involved in the adsorption of propylene [14,31,34]. Early studies on the effect of the support showed that isolated and/or highly dispersed tetrahedral titanium sites can be obtained in either mesoporous titanosilicate (TiO_2-SiO_2) or microporous titanosilicate (TS-1). Well dispersed titanium-containing supports result in catalysts more resistant to deactivation and able to obtain slightly higher PO yields in spite of the low propylene conversion values achieved (Table 1) [35]. However, these tetrahedral sites together with neighbouring surface hydroxyl groups (Ti-OH, Si-OH) are found to be responsible of the readsorption of PO [36], which further causes catalyst deactivation by producing bidentate propoxy species, carbonates, carboxylates, and oligomers on the catalyst surface [13–17,30,35–38]. Accordingly, it was observed that deactivation with time on stream occurs even when nonporous silica was used as a major carrier of Au catalysts [39,40], indicating that both the surface properties and the hydrophobic character rather than steric structure of the Ti-containing supports are related to the deactivation. Further confirmation of the effect of silanol sites (Si-OH) in the catalyst deactivation [17,38,39,41–43] was given by Qi et al. [44] who observed by IR and HRTEM analyses that the interaction between titanium oxides and commercial non-porous silica can be intensified to form more isolated TiO_4 units with tetrahedral coordination with an increase in heat treatment temperature, diminishing catalyst deactivation. Likewise, the deactivation of Au/TiO_2-SiO_2 catalysts can be controlled by adding trimethylamine in the reaction feed [41,45], since in this way, silanol sites could be masked. Similarly, Nijhuis et al. [46] observed that the presence of water in the feed gas stream can also suppress the catalyst deactivation by lowering the PO concentration adsorbed on the titania through competitive adsorption, however, an associated small decrease in the catalytic activity is also observed as a side effect.

Consequently, in order to obtain highly active and stable catalysts, it is important to optimise the Ti/Si ratio in the support to get a compromise between tetrahedral Ti dispersion and deactivation caused by silanol groups. Interestingly, a volcano-type effect of the Ti/Si ratio on the propylene conversion is observed while the PO selectivity decreases linearly with the Ti/Si ratio (Fig. 1).

The superior performance in terms of propene conversion, PO selectivity and H_2 efficiency in comparison with the Au catalysts supported on conventional Ti-containing mesoporous materials were reported by Yang et al. [43], who studied the performance of Au/Ti-HMS (titanium-containing hexagonal mesoporous silica). This fact was ascribed to the homogeneous distribution and uniformity of titanium species in combination with the accessible pore structure. Similarly, Xu et al. [48] used a hybrid material composed of a core TS-1 zeolite particle surrounded by a shell of mesoporous silica-gold nanoparticles which is not only more robust against catalytic deactivation but also more selective to PO than Au/TS-1 catalysts.

As previously stated, the support is also partially responsible (in addition to the gold loading method) for the dispersion level of the metal nanoparticles. Consequently, few studies have used high-surface area mesoporous supports for the tandem system.
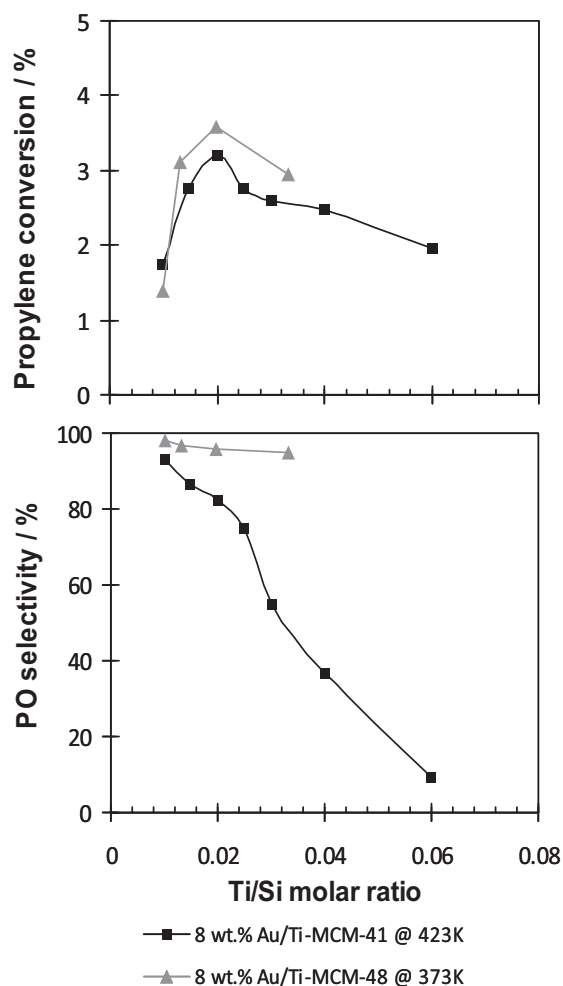

Fig. 1. The effect of the Si/Ti ratio of the support on the propylene conversion and PO selectivity [37,47].

Indeed, gold nanoparticles on Ti-modified mesoporous supports such as MCM-41, MCM-48, TUD-1 and SBA-15 has been observed to improved PO yields [37,47,49–54]. For example, Kalvachev et al. [52] studied the vapour-phase epoxidation of propylene over Au deposited on Ti-MCM-41 confirming the improved performance of mesoporous supports with respect to TiO_2-SiO_2 mixed oxides. The performance of gold particles deposited on the Ti-MCM-41 and Ti-MCM-48 supports were compared by Uphade et al. [37], who observed a better performance for the Ti-MCM-48. This fact was ascribed to its three-dimensional pore system. At the same time, Qi et al. [39] found that Au/Ti-MCM-41 type amorphous support is one order of magnitude more active than Au/Ti-MCM-48 in terms of both the PO formation rate per unit weight of Au and of hydrogen efficiency. Both studies are not directly comparable as different reaction conditions are used.

Sacaliuc et al. [54] synthesised Au/Ti-SBA-15 using two different Ti-SBA-15 supports synthesised by Ti-grafting and direct synthesis concluding that those materials obtained by Ti grafting had greater catalytic activity, which was ascribed to an increase in the amount and dispersion of Ti within the mesoporous silica support. Consequently, it influences the final Au nanoparticle size, emphasising the advantage of using high surface area silica supports for this reaction.

The treatment of the support prior to metal loading has also been explored as a strategy to increase the conversion of propylene whilst keeping the selectivity to PO. Thus, Sacaliuc-Parvulescu et al.

Table 1
Review of the different Au-based catalytic systems used for the epoxidation of propylene with *in-situ* generated H_2O_2.

Ref no	Catalyst			Experimental conditions				Activity results			Reaction rate	
	Support	Au loading	Au particle size	Mass catalyst	T	GHSV	C_3H_6:H_2:O_2:Inert	Propylene conversion	PO selectivity	H_2 efficiency		
		wt%	nm	g	K	N mL g cat^{-1} h^{-1}		mol%	mol%	mol%	gPO h^{-1} kg cat^{-1}	mol PO h^{-1} Au mol^{-1}
[35]	TiO$_2$	1	3–10	0.3	323	110	1:1:1:7	0.8	99	–	5.4	1.83
[31]	TiO$_2$	1		0.3	323	10,000	1:1:1:7	0.2	99	–	4.8	1.62
[46]	TiO$_2$	1		0.3	398	9000	1:1:1:7	0.1		–	0.0	0.00
[22]	TiO$_2$	1	4.2	0.35	323	8571	1:1:1:7	0.2	99	12.2	4.7	1.6
[29]	P25 TiO$_2$	1	3.7		323	6000	1:1:1:7	0.9	99	–		
[32]	TiO$_2$	1		0.3	323	10,000	1:1:1:7	0.1	99	–	2.4	0.8
[41]	TS-1	3.5	2.5		433	4000	1:1:1:7	5.0	89	–	42.8	4.16
[44]	TiO$_2$-SiO$_2$	0.36	2.8	0.5	333	4000	1:1:1:7	0.08	99	–	0.8	0.7
[26]	TiSiO$_2$	1		0.02	394	9990	1:1:1:7	0.7	99	14	17.4	5.9
[45]	Ba promoted TiO$_2$-SiO$_2$	–	–		423	4000	1:1:1:7	8.5	91	35	74.5	–
[77]	Au-Pd/TiO$_2$-SiO2	–	–	0.2	423	13,500	0.83:0.84:0.83:7.5	6.1	2.9	–	6	–
[43]	Ti-HMS	0.61	4.2	0.15	373	4000	1:1:1:7	9.0	97.3	30.4	84.3	46.9
[25]	Ti-HMM	0.3	–	0.15	393	4000	1:1:1:7	4.2	94.3	–	38.1	43.2
[33]	grafted Ti	0.06	–		473	10,000	1:1:1:7	2.4	89.4	20.6	0.0	0.10
[60]	Ti-MCM-48 (CsNO$_3$ promoter)	0.4	3.5		523	4000	1:2:1:6	3.0	70.4	–	20.5	17.4
[17]	Ti-MCM-41	2	2.7	0.15		4000	1:1:1:7	2.4	94	16	21.7	3.7
[39]	Ti-MCM-41	0.019	–	0.3	473	4000	1:1:1:7	1.1	90	–	10.5	187
[52]	TiO$_2$/Ti-MCM-41	1.2	2	0.5	373	4000	1:1:1:7	1.5	96	–	13.9	3.92
[47]	Ti-MCM-41	1	2.2	0.5	373	4000	1:1:1:7	3.1	92	–	27.5	9.3
[57]	Ti-MCM-41	0.18	–	0.15	423	4000	1:1:1:7	2.2	96	–	20.3	38
[40]	TiO$_2$-SBA15	0.25	<2	0.1	353	15,000	1:1:1:7	0.4	99	19.1	15.7	21.4
[54]	Ti-SBA15	1	2.8	0.4	393	7500	1:1:1:7	0.5	96.5	9.23	8.4	2.84
[51]	Ti-SBA15			0.4	408	7500	1:1:1:7	0.8	97.7	3.27	14.1	–
[63]	Ti-TUD-1 C.2-1	0.31	–	0.15	373	8000	1:1:1:7	0.8	89	–	13.2	14.5
[63]	Ti-TUD-1 C.2-3	0.31	4.3	0.15	373	8000	1:1:1:7	1.3	76	–	25.0	27.4
[53]	TiTUD	0.11	0.9	0.3	423	7000	1:1:1:7	1.4	99.6	17.2	23.5	72.5
[27]	Ti-TUD-1 (Ba promoted)	0.11	–	0.3	423	7000	1:1:1:7	1.2	99	16	20.0	61.8
[49]	TS-1 2% Ti (silylated)	0.35	3	0.4	433	4000	1:1:1:7	3.8	96.4	34	35.3	34.2
[55]	TS-1	0.058	–	–	473	7000	1:1:1:7	5.0	83	–	69.9	409.5
[61]	TS1	0.33	3.5	0.3	473	7000	1:1:1:7	9.7	87	–	142.2	146.35
[56]	TS-1 (Si/Ti = 99)	0.146	–	0.15	473	14,000	1:1:1:7	8.6	92	10.7	154	357
[23]	TS-1 (Si/Ti = 36)	0.05	–	0.3	473	7000	1:1:1:7	8.8	81	–	120.1	815.85
[62]	TS-1_120	0.25	2.5	–	413	7000	1:1:1:7	3.9	90.9	–	59.7	81.2
[65]	TS1 (Ge promoted)	0.22		0.3	443	7000	1:1:1:7	4.0	91	–	61.3	94.7
[64]	TS-1	10	3.3	0.3	398	6600	1:1:1:7	3.5	80	–	44.5	1.51
[58]	TS-1	0.5	3.4	0.15	573	4000	1:1:1:7	9.6	74.5	26.8	68.9	46.78
[127]	S-1/TS-1	0.054	3	–	423	14,000	1:1:1:7	0.6	99	38	11.0	69.19
[48]	TS-1 encapsulated on SiO$_2$	0.2	–	0.3	423	4000	1:1:1:7	2.6	94.4	–	23.6	40.1

[51] studied the effect of the ammonium treatment of the Ti-SBA-15 support on the catalyst performance, observing a 10 times increase in the PO formation rate. The presence of amine species favours the homogeneous distribution of gold nanoparticles favouring both the *in-situ* synthesis of hydroperoxo species and the posterior epoxidation. The same effect was observed over the ammonia-treated TS-1 support. In this case, the ammonia treatment results in a fourfold increase of the Au capture efficiency, leading to turnover numbers above 400 mol PO Au mol^{-1} h^{-1} at 200 °C [55].

2.2. The effect of the metal

As mentioned above, gold supported over Ti-based materials are the most studied systems in the propylene epoxidation reaction (Table 1). The effect of gold size on the epoxidation of propylene has been scrutinised in numerous studies. Interestingly, Hayashi et al. [11] demonstrated that the reaction pathway can be tuned by carefully controlling the size of the gold particles. Gold particles larger than 2 nm produce PO whereas smaller sized gold particles turn into propane. Conversely, an optimum gold size of ∼1 nm is reported by Lee et al. [56]. In any case, the effect of gold size becomes more complex in the tandem *in-situ* hydrogen peroxide synthesis and its one-pot use for propylene epoxidation.

Metal nanoparticle size is well known to be directly related to the loading method used in catalyst preparation. The deposition–precipitation (DP) method was used to synthesise gold supported on a Ti-containing silicate mesoporous material (TUD-1) for the direct epoxidation of propylene with H$_2$ and O$_2$ mixtures [53]. It was observed that increasing the pH of the deposition of gold nanoparticles decreases not only the final gold loading and but also its particle size in the catalyst, and consequently increases the selectivity to PO. Hydrogen selectivity also increased with increasing pH of preparation as gold particles with sizes above 2 nm are found to be active in the decomposition of H$_2$O$_2$ to water. A similar effect is obtained when using TS-1 as a support (Fig. 2). Low gold loadings and small gold particle sizes (around 1 nm) seems to be the most selective systems for H$_2$ efficiency and PO formation in the tandem H$_2$O$_2$ synthesis–epoxidation reaction [56]. In general, a direct relationship between pH during the deposition–precipitation method and the PO turnover number is observed except at high pH values (>8.5) when the reactivity decreases. In these cases, the catalysts present partially oxidised Au species while those prepared at lower pH values contain mainly metallic gold. This observation is in agreement to that reported by Sinha et al. [57] for systems using a Ti-MCM-41 mesoporous support. They studied the influence of gold loading and speciation in
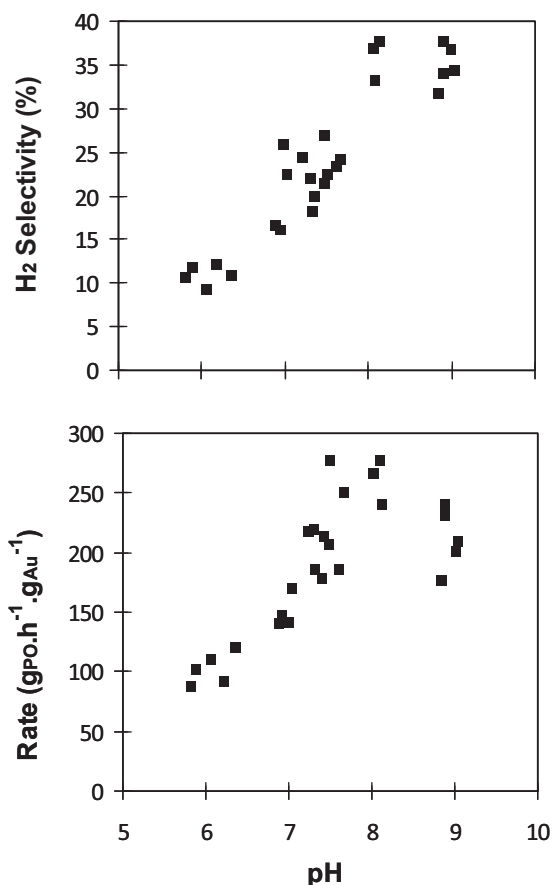

Fig. 2. The effect of pH during the deposition–precipitation method of gold nanoparticles on a TS-1 support on the final gold loading, PO rate and H$_2$ selectivity [56].

the selectivity to PO concluding that the presence of metallic gold results in a higher epoxidation selectivity.

A different alternative approach was developed by Zhan et al. [58,59] to deposit Au on TS-1. These authors applied a bio-reduction method to load Au using plant extract leading to an increase in propylene conversion and H$_2$ efficiency (48.9%).

The effect of different promoters in the catalytic system has also been studied by a series of authors. Wang et al. [60] observed that the impregnation with inorganic salts such as CsNO$_3$ over Au/Ti-MCM-48 catalysts could promote the epoxidation of propene to PO whereas KBr led to the production of propionaldehyde. Similarly,

Table 2
Review of the different Ag, Pd and Pt catalytic systems used for the epoxidation of propylene with *in-situ* generated H$_2$O$_2$.

Ref no	Experimental conditions					Activity results	
	Catalyst	Mass catalyst g	T K	Space velocity	C$_3$H$_6$:H$_2$:O$_2$:Inert	Propylene conversion mol%	PO selectivity mol%
[67]	Ag/TS-1	0.6	423	3000 h^{-1}	1:2:3:8	0.9	91.2
[68]	Ag/TS-1 (precipitator: Cs$_2$CO$_3$)	0.6	423	4000 h^{-1}	1:2:3:12	1.3	84.1
[69]	Ag/TS-1	0.6	423	4000 h^{-1}	1:2:3:12	1.3	93.5
[68]	Ag/TS-1	0.6	423	4000 h^{-1}	1:2:3:12	0.4	92.7
[75]	Titanosilicates Pd-NHTS	1	na	na	1:1.2:1.2:–	1.9	91.5
[20,76]	Pd/TiO$_2$	0.5	room	na	2:1:2:5	2	30–60
[12,66]	Pd-Pt/TS-1	0.2	316	na	–:7:10:15	26.1	6.6
[71]	Pd-Pt/TS-1	0.2	na	4.1 NL g^{-1} h^{-1}	1:13:13:14	21	71
[72]	Pd-Pt/TS-1		316	na	na	–	–
[19]	Pd-Pt/TS-1	0.05	333	na	1:1:1:–	28.7	81.8

Sinha et al. [49] demonstrated that highly dispersed gold nanoparticles can be obtained when $Ba(NO_3)_2$ was used as a promoter prior to metal loading [61]. Lu et al. [62] studied a series of Au/TS-1 catalysts promoted with alkaline and alkaline earth cations. They found that the addition of Group 1 metals (K, Cs) has little effect on the gold loading but increases the catalytic activity. Group 2 metal promoters (Mg, Ca, Sr, Ba) increase both gold content and catalytic activity, Mg showing the highest effect. Additionally, Qi et al. [63] demonstrated the effect of the presence of alkali cations on promoting the epoxidation reaction to PO *versus* hydrogenation towards propane. The incorporation of cobalt during the preparation also increases the Au uptake of the support and increases its stability *versus* deactivation [64]. On the other hand, the presence of Ge on Au/TS-1 catalysts improves both propylene conversion and selectivity to PO due to a decrease of the activation energy of the epoxidation reaction caused by the ligand effect of Ge on the Ti active sites [65].

Although to a lesser extent, the effect of other precious metals apart from gold has been also reported over either titania or titania-silicate supports. Lower propene conversion and poorer PO selectivity have been found compared to the gold-based systems [12,19,20,66–76] (Table 2). Specifically, Ag/TS-1 catalysts have been studied by different authors [67–70]. Contrary to the gold case, oxidised silver ions are the main active sites improving the selectivity to PO by the presence of framework titanium species. Optimum preparation conditions to achieve both high propelyne conversion and high selectivity to PO were investigated by Wang et al. [68]. They found that the most efficient catalyst was synthesised by a deposition-precipitation method with a resulting silver loading of 2 wt% in a support with Si/Ti ratio of 64. These authors also reported that the use of K_2CO_3 as a precipitator improved the stability and selectivity whilst Cs_2CO_3 enhanced the catalyst stability [68]. Oxidised palladium (II) species in small clusters are also favourable for the formation of PO compared to fully reduced Pd species and large clusters selective to hydrogenation to propane. Metal alloys have also been studied as active sites for this tandem process. In Pd-Pt/TS-1 catalysts, the addition of 0.01–0.02 wt% Pt increases the fraction of Pd(II) species achieving maximum PO yield and selectivity [12]. Jin et al. [77] prepared a compact zeolite membrane of TS-1 on the surface of $Au-Pd/TiO_2-SiO_2$ catalyst pellets. This material showed much higher propylene conversion and PO yield than those of the conventional physically mixed catalyst with the same composition.

2.3. The effect of the reaction temperature

Despite the inherent difficulties of comparing catalytic data obtained at different reaction conditions, general trends can be drawn related to the effect of the reaction temperature in the overall conversation and selectivity of the tandem system. As expected, the conversion of propylene increases as the reaction temperature increases mirroring the increase in the rate of the reaction. Contrarily, the selectivity towards propylene oxide decreases as the temperature increases. It is worth mentioning that 100% selectivity to PO can be achieved at relatively high temperatures (<400 K) depending on the catalytic system (Fig. 3), however, the hydrogenation to propane and its complete oxidation to CO_2 and water are favoured at high temperatures dramatically decreasing the selectivity to PO [63]. Additionally, the hydrogen efficiency decreases as the temperature increases as the parallel decomposition of *in-situ* generated hydrogen peroxide to water increases. As mentioned before, this parameter is normally used to assess the economic feasibility of the system, and therefore, it should be a priority when designing catalysts for the direct epoxidation of propylene with hydrogen and oxygen mixtures.
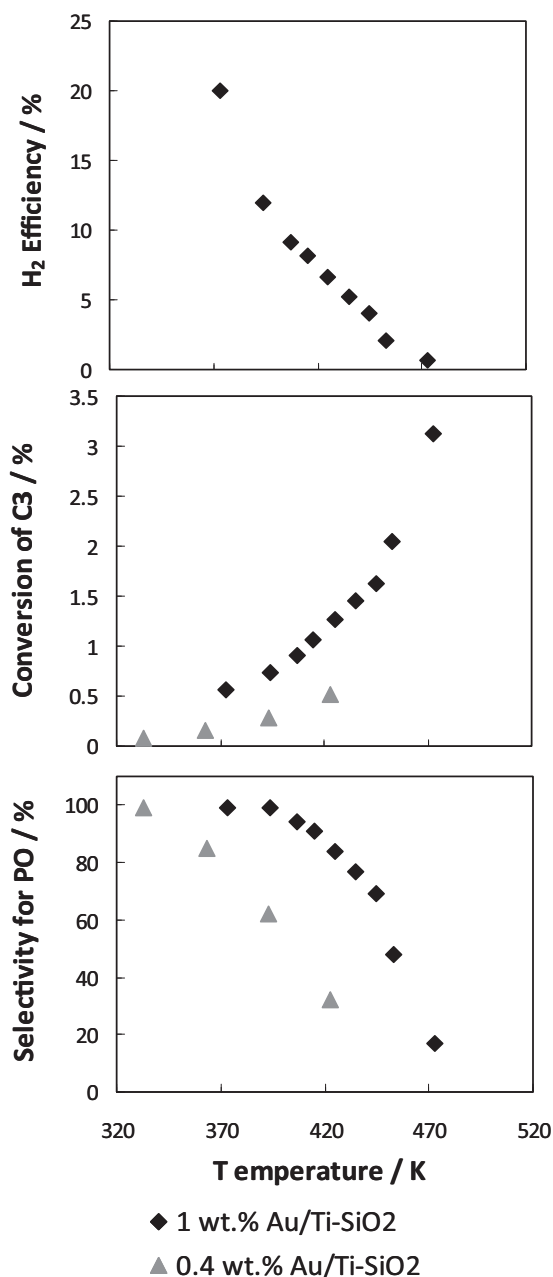

Fig. 3. The effect of the reaction temperature on the conversation of propylene, selectivity to PO and overall H_2 selectivity [26,44].

3. Hydroxylation of benzene to phenol

Phenol is an important intermediate in the chemical industry for the synthesis of drugs, functional polymers and dyes, amongst others. Currently, phenol is produced at large scale from benzene using the so-called Cumene process. This three-step highly energy intensive process leads to low phenol yields with a high production of by-products, mainly acetone and methylstyrene. Different options to this process have been proposed such as the use of nitrous oxide as an oxidant [78]. Alternatively, the direct hydroxylation of the benzene aromatic ring with molecular oxygen and hydrogen has also attracted great interest as a green route for this transformation (see Table 3).

Remias et al. [79] reported the mechanistic insights of the hydroxylation of benzene and cyclohexane using *in-situ* generated hydrogen peroxide from oxygen and hydrogen with palladium

Table 3
Performance of the different catalytic systems in the hydroxylation of benzene to phenol using *in-situ* generated H_2O_2.

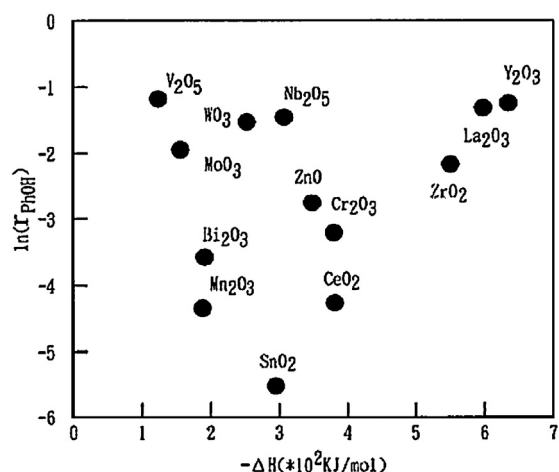| Ref no	Catalyst	Experimental conditions						Catalytic results		
		System	Benzene mL	Mass catalyst g	T K	GHSV N mL g$_{cat}^{-1}$ h^{-1}	H$_2$/O$_2$ ratio	Benzene conversion mol%	Phenol selectivity mol%	Reaction Rate g$_{phenol}$ g$_{cat}^{-1}$ h^{-1}
[80]	Pd-Cu composite catalyst supported on silica	Semi-batch	100	2	298	450 N mL g cat^{-1} h^{-1}	1	2	na	0.0034
[82]	Pd and Cu supported on silica gel	Continuous	20	2	413	1287 N mL g$_{cat}^{-1}$ h^{-1}	1	na	na	0.003
[81]	Pt/V$_2$O$_5$-SiO$_2$	Semi-batch	20	1	333	1928 NmL g$_{cat}^{-1}$·h^{-1}	2.9	na	100	0.109
[84]	Pt/V$_2$O$_5$-SiO$_2$	Continuous	2	0.25	298	450 N mL g$_{cat}^{-1}$ h^{-1}	1	97	na	0.028
[79]	Pd/V(Acac)$_3$-Al$_2$O$_3$	Batch	2	0.02	298	–	1	14	99	0.94
[87,88]	Pd-Pt/Nafion/silica composites	Batch	2.3	0.2	316	–	1	4.3	99	0.17

Fig. 4. The effect of the metal oxide promoter (20 wt%) on a 0.5 wt% Pd/silica catalyst on the rate of phenol formation. Reprinted with permission from [81].

nanoparticles supported on vanadium and iron oxides. The study indicates that the rate limiting step of the overall system is the formation of H_2O_2. An electron transfer mechanism with a radical cation intermediate was proposed for the benzene hydroxylation by vanadium or iron oxide which is not affected by the presence of metallic palladium.

3.1. The effect of metal and redox promoters

Group VIII metals have been generally used for the direct synthesis of phenol with hydrogen and oxygen mixtures. Negligible or relatively small phenol yields are obtained when only metals are used in the absence of redox promoters [80]. As an example, Miyake et al. [81] demonstrated the direct formation of phenol over Pd, Rh, Ir and Pt supported on silica, however, with an extremely small selectivity compared to water production. Conversely, it was observed that if the catalyst is modified with vanadium oxide, the phenol formation is significantly improved more than fifteen times. Consequently, a series of redox promoters (metal oxides) have been considered to increase phenol yield such as vanadium, wolframium, molybdenum, niobium, zinc, bismuth, manganese, tin, cerium, zirconium, chromium, lanthanum and yttrium oxides. Fig. 4 shows the effect of different main metal oxides in the rate of formation of phenol, directly related to hydrogen yield. Vanadium oxide was generally found as the most effective promoter, Y_2O_3 and La_2O_3 being also very efficient to promote benzene hydroxylation (Table 3). Interestingly, a similar enabling effect is observed with a Pd/Cu composite catalyst supported on silica, compared to the inactive Pd-only system, revealing the essential role that the Cu$^{I/II}$ redox couple played in the reaction [80]. Specific to this system, Kitano et al. [82,83] highlighted the importance of the catalysis preparation method showing that if Pd was loaded by means of ion-exchange instead of impregnation, the performance of the Pd-Cu composite was nearly doubled.

The role of the promoter is believed to be related to the inhibition of the parallel decomposition of hydrogen peroxide reaction on the surface of the metals. In this way, oxygen adsorbed on monomeric vanadium species is transferred to the metallic sites, increasing the relative amount of oxygen on the surface of the metal which prevents the over-hydrogenation of the *in-situ* generated H_2O_2. As a result, a higher concentration of H_2O_2 is present in the system, increasing not only the rate of phenol formation but also the hydrogen yield. Moreover, the metal oxide promoters might also have an effect on the dispersion of the precious metals over the support, leading to smaller particle sizes with higher reactivity
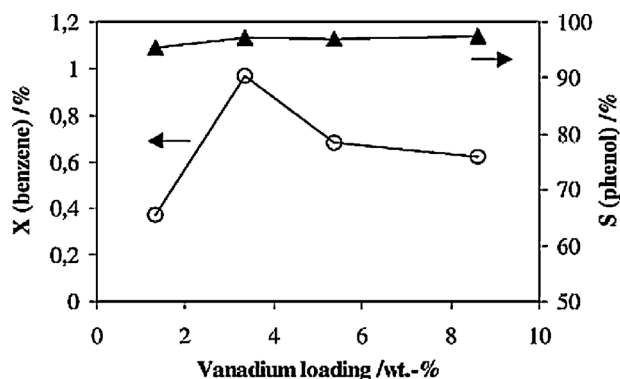
Fig. 5. The effect of vanadium oxide loading on the conversion of benzene and phenol selectivity. All catalysts are 0.5 wt% Pt-V/SiO_2. Reprinted with permission from [84].

Fig. 6. The effect of the H_2/O_2 molar ratio on the phenol yield in membrane reactor systems. ■: Sputtercoated Pd membrane [94]; ▲: Pd membrane on TS-1 and α-Al_2O_3.

towards hydrogen peroxide synthesis. Accordingly, Ehrich et al. [84] show the effect of the metal to promoter ratio (Fig. 5) on the final benzene conversion and phenol yield. In their case, the best reactivity is achieved with a low metal loading (0.5 wt% Pt) and a V/Pt ratio of 6. Therefore, optimum catalysts require both a high dispersion of the transition metal oxide and small metal particles.

3.2. The effect of the support

Despite silica being the most common support for this tandem process, the literature contains scattered studies using other supports. For example, Tatsumi et al. [85] studied a palladium supported on TS-1 catalyst and demonstrated the enhanced properties of TS-1 for selective hydroxylation of aromatics using *in-situ* generated hydrogen peroxide, showing an increase of both benzene conversion and phenol selectivity [86]. Resins like Amberlyst or Nafion/silica composites have also been explored as supports to carry out the direct benzene hydroxylation [87,88]. Optimum results are obtained over a strong acidic Nafion/silica composite carrier with 13% Nafion containing 0.5 wt% Pd and 0.5 wt% Pt due to a combination of strong acidic properties, high dispersion of the Nafion resin on the silica matrix and its hydrophobic/hydrophilic properties. Despite this, low phenol selectivity values of *ca* 41% are reported, being hydroquinone, the main by-product.

3.3. Membrane reactors

Membrane reactors have been significantly used in this tandem process by a series of authors [86,89–99]. Generally, a Pd-based membrane is used to separate feed streams on both sides of the membrane. On one side, hydrogen is fed into the system while a mixture of benzene and oxygen is introduced in the other side of the membrane. Hydrogen permeates through the metallic membrane following a three-step mechanism: (i) dissociative adsorption of hydrogen into atoms, (ii) diffusion of the hydrogen atoms through the octahedral interstitial sites of the face-centreed cubic palladium lattice and (iii) associative desorption of molecular hydrogen, however, in these kind of tandem systems, permeated hydrogen atoms are believed to react with oxygen before recombination to produce different active oxydant species such as HOO•, HO• and H_2O_2 *in-situ* used for the hydroxylation of benzene [86,90]. While HOO• and HO• can be expected to be short lived and localised on the surface of the Pd membrane, H_2O_2 can diffuse from the membrane to the catalyst [86,90]. Despite the obvious advantages of these membrane reactors in terms of safety, avoiding direct contact of oxygen and hydrogen, phenol yield and hydrogen efficiency remain
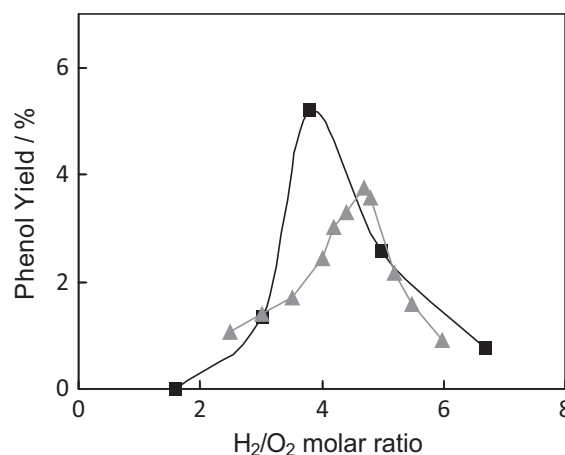
as challenges (Table 4). Generally, a large amount of by-products (CO_2 and H_2O) from side reactions are produced whereas the formation of phenol is relatively very low. Over-oxidation of benzene into CO_2 can be caused by the highly oxidative species formed on the Pd membrane. On the other hand, the hydrogen utilisation efficiency decreases due to the excess of hydrogen (respect to oxygen) in the membrane surface, being the production rate of water 500–1000 times higher than that of phenol. Further optimisation of the process and the reaction conditions have been carried out in order to enhance both yields. Thus, Sato et al. [92] demonstrated the importance of the reaction atmosphere: while oxygen-rich conditions can cause the complete oxidation to CO_2, high hydrogen flux induce hydrogenation activity and consequently, water formation. In general, a balance of the H_2/O_2 ratio needs to be achieved to maximise the phenol yield obtained as shown in Fig. 6.

Additionally, the reaction temperature plays a vital role in the membrane systems beyond its effect on the reaction due to the thermal membrane stability. Palladium embrittlement takes place below 573 K, initially producing pitch holes in the membrane before its complete rupture due to $\alpha \rightarrow \beta$ phase transition [93]. To avoid this, Pd-alloy membranes are normally used [100]. Specifically, Pd-Cu membranes where used in a double membrane reactor, reaching a phenol selectivity of 67% [97]. A complement engineering approach is the use of membrane microsystems to control the localised H_2/O_2 ratio [94,95].

However, to compete with the commercial well-established Cumene process for large-scale production of phenol, an increase of the overall benzene conversion while keeping high selectivity to phenol, the reduction of the cost of the metallic membrane and its long-term performance, remain important issues to deal with in the near future.

4. The selective oxidation of methane into oxygenates

One of the great challenges in the field of selective oxidation is the direct transformation of methane (the primary component in natural gas) into oxygenates. Currently, a two-step highly energy intensive process is used where the activation of the C–H bond takes place at high temperatures to form syn-gas prior its further conversion into oxygenates. Evidently, economic and environmental advantages can be gained through the direct oxidation of methane into oxygenates in a single step with careful control of the over-oxidation of the oxygenated products into CO_2. Pioneering studies in the field used concentrated acids, such as H_2SO_4, with Pt-based catalysts [101,102], however, a breakthrough from the environmental point of view is the use of green oxidants

Table 4
Performance of the different catalytic systems in the hydroxylation of benzene to phenol using *in-situ* generated H_2O_2 in membrane reactors.

Ref no	Membrane system	Experimental conditions				Catalytic results		
		System	T K	GHSV	H_2/O_2 ratio	Benzene conversion mol%	Phenol selectivity mol%	H_2 efficiency mol%
[86]	Pd/TS-1 membrane reactor	Continuous	473	na	>2.5	6	95	
[89]	Pd membrane reactor	Continuous	433	15,977 mL cm$_{Pd}$$^{-2}$ h^{-1}	0.7	9	70	0.2
[90]	Pd membrane reactor	Continuous	473	na	4.6	9	70	0.3
[91]	Pd membrane reactor	Continuous	423	1692 mL cm$_{Pd}$$^{-2}$ h^{-1}	4.5	4	4	0.3
[92]	Pd membrane reactor	Continuous	423	7105 mL cm$_{Pd}$$^{-2}$ h^{-1}	4	16	95	
[93]	Pd membrane reactor	Continuous	423	71 mL cm$_{Pd}$$^{-2}$ h^{-1}	4	0.15	80	0.64
[94]	MEMS-based Pd microreactor	Continuous	473	2859 mL cm$_{Pd}$$^{-2}$ h^{-1}	4	55	36	9.1
[98]	Pd-TS-1 membrane reactor	Continuous	473	2859 mL cm$_{Pd}$$^{-2}$ h^{-1}	4.7	4	73	25
[95]	Pd-Cu-double membrane micro-reactor	Continuous	423	5 mL cm$_{Pd}$$^{-2}$ h^{-1}	1.4	0.015	8	na
[96]	Pd/silicalite-1 composite membrane	Continuous	473	na	4.7	5	61	na
[97]	Pd-Au membrane reactor	Continuous	423	5 mL cm$_{Pd}$$^{-2}$ h^{-1}	1	0.02	68	0.01

such as H_2O_2 [103]. Following the lines of this review, further advantages can be obtained with *in-situ* generated hydrogen peroxide or peroxo species (Table 5). Lin et al. [104] selectively oxidised methane, ethane and butane in the presence of oxygen and carbon monoxide on a mixture of trifluoroacetic acid and water using Pd/C and copper chloride as a catalytic system. The proposed mechanism shown in Fig. 7, involves a metal catalysed water gas shift reaction and the subsequent formation of H_2O_2. Further experiments suggest that the principal role of metallic palladium was to generate hydrogen peroxide *in-situ*, being the copper chloride species responsible for the hydroxylation of the hydrocarbons into their corresponding alcohols [73,105].
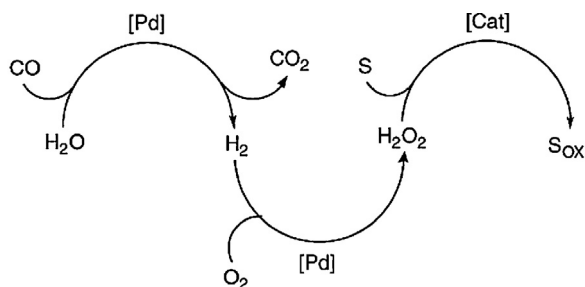
A similar catalytic system was studied by Park et al. [106] who observed that in the presence of copper chloride, the metallic palladium can be partly oxidised into Pd(II) species, responsible of the selective activation of methane and the formation of CF_3COOCH_3 and formic acid. On the other hand, metallic palladium remains key for the *in-situ* formation of H_2O_2. Heteropoly compounds such as $Pd_{0.08}Cs_{2.5}H_{0.34}PVMo_{11}O_{40}$ have also been explored as an alternative. In these cases, the formation of hydrogen peroxide is believed to be catalysed by Pd with acidic sites in the heteropoly

Table 5
Performance of the different catalysts in the selective oxidation of methane into oxygenates using *in-situ* generated H_2O_2.

Refno	Catalyst	Main Products	System	T K	Time	Gas Phase	Activity results
[106]	5% Pd/C and Cu(CH$_3$COO)$_2$	CF$_3$COOCH$_3$ and formic acid	Batch	473	5 h	CH$_4$ = 20.7 bar; N$_2$ = 6.9 bar; CO = 13.8 bar; O$_2$ = 6.9 bar	CF$_3$COOCH$_3$ production: 13.8 mol mol$_{Pd}$$^{-1}$ h^{-1} HCOOH production: 12.4 mol mol$_{Pd}$$^{-1}$ h^{-1}
[110]	1% Pd/C and tetrachlorobenzoquinone	CF$_3$COOCH$_3$ and formic acid	Batch	413	3 h	CH$_4$ = 17.8 bar; CO = 9.9 bar; O$_2$ = 5.0 bar	CF$_3$COOCH$_3$ production: 93 mol mol$_{Pd}$$^{-1}$ h^{-1}, HCOOH production: 32.3 mol mol$_{Pd}$$^{-1}$ h^{-1}
[108]	5% Pd/C and Cu(CH$_3$COO)$_2$	CF$_3$COOCH$_3$ and formic acid	Batch	353	10 h	CH$_4$ = 34.1 bar; H$_2$ = 6.8 bar; O$_2$ = 6.8 bar	CF$_3$COOCH$_3$ production: 8 mol mol$_{Pd}$$^{-1}$ h^{-1}, HCOOH production: 5.2 mol mol$_{Pd}$$^{-1}$ h^{-1}
[109]	5% Pd/C and Cu(CH$_3$COO)$_2$	CF$_3$COOCH$_3$ and formic acid	Batch	353	5 h	CH$_4$ = 34.1 bar; H$_2$ = 6.8 bar; O$_2$ = 6.8 bar	CF$_3$COOCH$_3$ production: 10.4 mol mol$_{Pd}$$^{-1}$ h^{-1}, HCOOH production: 3.2 mol mol$_{Pd}$$^{-1}$ h^{-1}
[104]	5% Pd/C and CuCl$_2$/K$_2$PdCl$_4$	Methanol	Bath	356	18 h	CH$_4$ = 69 bar; CO = 13.8 bar; O$_2$ = 6.9 bar.	Methanol formation: 0.89 mol mol$_{Pd}$$^{-1}$ h^{-1}
[111]	RhCl$_3$	Methanol and methyl ester	Bath	353	80 h	CH$_4$ = 69 bar; CO = 20.7 bar; O$_2$ = 6.9 bar.	Me-ester production: 2.3 mol mol$_{Rh}$$^{-1}$ h^{-1}, AcOH production: 0.5 mol mol$_{Rh}$$^{-1}$ h^{-1}
[107]	Pd$_{0.08}$Cs$_{2.5}$H$_{0.34}$PVMo$_{11}$O$_{40}$	Formic acid	Continuous	373	GHSV = 11,000 mL g$_{cat}$$^{-1}$ h^{-1}	CH$_4$ = 28%; H$_2$ = 33%; O$_2$ = 14%	CH$_4$ conversion: 0.077%, Selectivity to HCOOH: 85%

Table 6
Performance of the different catalytic systems in the Fenton process using *in-situ* generated H_2O_2.

Ref no	Catalyst	Experimental conditions	Activity results
[116]	Pd/Al_2O_3	Phenol (100 ppm), ferrous iron (10 ppm), 0.1 g catalyst. Formic acid (40–500 mM). Oxygen flow rate = 20 ml min^{-1}.	Phenol degradation = 90%, Mineralisation degree = 57%
[117]	Pd/C	Rhodamine-B degradation	100% degradation of RhB at pH 2 after 30 min.
[115]	$Fe-Pd/Al_2O_3$	na	Phenol degradation = 93.2% after 6 h.
[118]	Fe/Pd-HTiNT	p-HBz oxidation (10^{-3} mol L^{-1}), 0.1 g catalyst, formic acid (FA) was injected into the reactor volume with nFA:npHBz = 2:1 molar ratio in UV light.	Mineralisation degree = 52%
[114]	$Fe-Pd/Al_2O_3$	Formic acid, hydrazine hydrate ($N_2H_4 \cdot H_2O$) and hydroxylamine sulphate ((NH_2OH)$_2 \cdot H_2SO_4$) in the presence of oxygen at 298 K.	Phenol degradation = 100% Mineralisation degree = 65%
[128]	$Fe-Pd/Al_2O_3$	Pentachlorophenol (PCP) and dichlorophenol (DCP) degradation @ 298 K (both simultaneous and consecutive reduction oxidation were studied over 6.5 h).	Chlorophenol degradation = 100% Mineralisation degree = 70% for DCP The consecutive reduction–oxidation protocol was the most efficient.

(S = substrate, S_{OX} = oxidized substrate, Cat = Pd or second catalyst)

Fig. 7. The mechanism for the selective oxidation of lower alkanes with *in-situ* generated H_2O_2. Reprinted with permission from [73].

compound while the hydroxylation takes place in the heteropoly compound itself [107].

Additionally, H_2/O_2 mixtures are more active than $O_2/CO/H_2O$ systems, as in the former case, the water gas shift reaction step is not required. Interestingly, in this case, a chlorine-free system can be used in combination with a heterogeneous Pd catalyst, where the presence of copper ($Cu(CH_3COO)_2$) remains essential for the activation of methane and metal palladium for the *in-situ* generated H_2O_2 [108]. Alternatively, the same research group used a series of vanadium compounds such as NH_4VO_3, $H_4PV_1Mo_{11}O_{40}$ or V_2O_5 to substitute the addition of copper [109]. Although copper-based catalysts are more active than vanadium ones, no difference in product yield was observed. In any case, the absence of copper or vanadium compounds leads to negligible amounts of oxidation products which means that hydrogen peroxide in the presence of Pd/C cannot drive the methane oxidation under these conditions. Similarly, the heavy metal copper can be replaced by p-tetrachlorobenzoquinone (TCQ) used in the industrial synthesis of H_2O_2 with similar roles in the catalytic system [110].

In addition to palladium-based systems, $RhCl_3$ along with several equivalents of Cl^- and I^- ions dissolved in an acidic solvent (mixture of perfluorobutyric acid and water) has also been studied for the direct oxidation of methane with CO/O_2 mixtures [111]. Selectivity towards methanol or acetic acid can be tuned by a simple change of solvent system. A curious aspect of the previous metallic Pd and the homogeneous Rh-based systems is that, apart from their ability to activate both dioxygen and the alkane, both require the presence of a co-reductant (carbon monoxide), showing a remarkable resemblance with the monooxygenases enzymatic system.

As an alternative to the addition of homogeneous co-catalysts, Hutchings et al. [112] have recently demonstrated the direct oxidation of methane to methanol over $AuPd/TiO_2$ catalysts using

either pre-formed hydrogen peroxide or *in-situ* generated from H_2 and O_2 mixtures. Interestingly, improved methanol selectivity is obtained in the latter case compared to the former with a similar productivity. Bimetallic $AuPd/TiO_2$ showed a remarkably higher productivity to methanol than a physical mixture of Au/TiO_2 and Pd/TiO_2 with the same metals loadings, showing once again the superior performance of AuPd alloy nanoparticles with unique catalytic properties. In this case, the primary product is methyl hydroperoxide which is believed to be formed by the reaction of H_2O_2 with $^\bullet CH_3$.

On a related study, Bravo-Suárez et al. [113] have studied the selective oxidation of propane to acetone and 2-propanol with a H_2 and O_2 mixture on Au/TS-1 catalyst. According to the spectroscopic results, H_2O_2 seems to be formed on the Au sites while propane is partially oxidised on Ti centres, demonstrating the formation of hydroperoxo species as true intermediates in the tandem reaction.

Despite the demonstration of the feasibility of the direct oxidation of methane into oxygenated products by *in-situ* generated H_2O_2, the productivities reported are still low and far away from values required for industrial application. Additionally, control of over-oxidation of the oxygenated products into worthless CO_2 remains a challenge for the future strategies to increase yields. Methane is the least reactive of the alkanes, thermodynamically more stable than its oxygenated counterparts (*e.g.* methanol) which tend to over-oxidise under reaction conditions. Further development of the bimetallic Au-Pd systems seems to have the potential to achieve high selectivity and high methane conversion at low temperatures. Additionally, engineering alternatives such as the use of membranes for a more controllable formation of hydrogen peroxide by H_2 and O_2 dosing might aid towards the medium term implementation of this system at large scale.

5. The Fenton process

Fenton systems are one of the cleanest and most efficient processes to eliminate particularly toxic compounds in both wastewaters and soil due to its ability to mineralise organic pollutants. The Fenton reaction involves the generation of a hydroxyl radicals ($OH^\bullet$) *via* hydrogen peroxide and ferrous ions. Recently, several groups have studied the one-pot process of this system in tandem with the *in-situ* generation of hydrogen peroxide normally using a combination of iron and palladium-based catalysts for both reactions respectively (Table 6). Contrary to previous processes, most of these studies avoid the use of potentially hazardous O_2/H_2 mixtures by using a series of H_2 substitutes, mainly formic acid, hydrazine and hydroxylamine [114–116]. Although hydrazine and hydroxylamine are, in general, more efficient as H_2 substitutes than formic acid for hydrogen peroxide formation, the controlled

production of H_2O_2 with O_2/formic acid mixtures results in more efficiency in terms of H_2O_2 utilisation when combined with the oxidation of organic pollutants. On the other hand, hydrazine/O_2 mixtures are highly efficient for H_2O_2 production at pH between 7 and 9 which can be highly advantageous when neutral or slightly basic effluents are treated [114]. Alternatively, hydrogen peroxide can be produced *in-situ* from electro-generated H_2 and O_2 using a Pd/C catalyst, as shown in the degradation of rhodamine B in an aqueous solution [117].

From a catalytic point of view, two different types of systems can be distinguished: (i) semi-heterogeneous, when a heterogeneous Pd-based catalyst is used for the *in-situ* generation of H_2O_2 and a homogeneous ferrous ion for the Fenton reaction and (ii) heterogeneous, when both Pd and Fe are supported. Although in both cases H_2O_2 is formed on the surface of Pd^0, in the semi-heteregeneous case, H_2O_2 is released into the solution where it is converted into $OH^\bullet$ radicals by the ferrous ions. On the other hand, in heterogeneous bi-metallic Pd–Fe systems, the *in-situ* generated H_2O_2 diffuses from the Pd^0 surface towards the Fe_2O_3 particle where radical formation occurs. Interestingly, Yalfani et al. show that a Pd–Fe alloy does not favour the Fenton reaction but a synergetic effect is observed by close conjunction with metallic Pd and Fe_2O_3 particles [115]. A variety of supports have been shown to be successful for this tandem system ranging from alumina [114,115], titanate nanotubes [118] and carbon [117]. Although its importance in the overall process is not fully elucidated, there are some indications in the literature of its potential role on the H_2O_2 diffusion in the heterogeneous case [115], apart from its obvious effect determining metal particle size as previously discussed.

Similarly, Osegueda et al. [119] prepared a catalytic membrane reactor with Pd impregnated on Fe_2O_3, $CuAl_2O_4$, TiO_2 or CeO_2 supports for the phenol oxidation reaction, demonstrating the viability for waste water treatment.

These studies clearly show the remarkable potential of *in-situ* generated hydrogen peroxide in waste treatment oxidation reactions, lowering the relevant current costs of H_2O_2 production. Additionally, it is important to highlight that the use of bi-metallic Fe-Pd catalytic systems not only to increase the degradation performance but also to decrease the environmental impact of the process by heterogenisation of the Fenton ferrous ion and its associated synergetic effects.

6. Oxidative desulphurisation

The permitted sulphur content in petrol and diesel fuels is continuously decreased by increasingly restrictive environmental regulations. The current method for sulphur removal from liquid fuel is mainly based on hydrodesulphurisation (HDS) which requires high temperature and pressure, making it a very costly option, especially for deep desulphurisation, to reduce the sulphur levels below 10 ppm. Based on this problem, there are many research and development efforts on alternative methods to eliminate the sulphur compounds from fuels, such as selective adsorption, alkylation, reactive desorption, bio-desulphurisation, oxidation/extraction (oxidative desulphurisation, ODS) or adsorption, *etc.* The development and application of oxidative desulphurisation are considered to be one of the most desired options due to its sulphur removal capability at mild conditions. Sulphides, such as thioether, thiophene and methylthiophene, which are primary organic sulphur components present in commercial gasoline, can be efficiently oxidised over TS-1, using hydrogen peroxide as an oxidant [120,121]. New research is now demonstrating the efficient removal of such components with *in-situ* generated hydrogen peroxide from H_2 and O_2 mixtures using metal supported on TS-1 based catalysts. Gold [122] and Pd [123]

supported on TS-1 seems to be the active species responsible for the direct synthesis of H_2O_2 whereas oxidation takes place on the Ti sites. Interestingly, a higher oxidation yield is achieved by Pd-modified titanosilicate compared to the impregnated counterparts [123]. Additionally, Song et al. [124] studied the oxidation of benzothiophene (BT) and dibenzothiophene (DBT) over Au/Ti-HMS catalysts observing almost 100% removal of sulphur with a higher stability after 5 consecutive cycles.

7. The oxidation of sulphides to sulphones

An interesting application of this tandem system is the *in-situ* generation of hydrogen peroxide for the selective oxidation of sulphides to produce sulphoxides and sulphones feedstocks for commodity chemicals and pharmaceuticals. Karmee et al. [125] reported for the first time the use of a supercritical CO_2/H_2O biphasic system for the *in-situ* generation of H_2O_2 from H_2 and O_2 and the chemoselective oxidation of thioanisole to methyl phenyl sulphone. Pd nanoparticles supported on SiO_2 was used for the first step while the oxidation takes place on TiO_2. Similar thioanisole conversions (99%) and selectivity to methyl phenyl sulphone (96%) values are obtained compared to the same system using pre-generated H_2O_2 as an oxidant [126].

8. Conclusions and future perspectives

Selective oxidation using *in-situ* generated hydrogen peroxide requires a two-step tandem process involving the generation of H_2O_2 on noble metals (mainly Au, Pd, Pt and bi-metallic combinations), normally from molecular oxygen and hydrogen, followed by its use in the oxidation of reactants into selected products, in most cases avoiding their over-oxidation into CO_2. Although in most cases a combination of two active sites are needed for each of the tandem steps, future catalytic development should focus on single active sites capable of undertaking both reactions in parallel to avoid diffusion limitations of the generated H_2O_2. Alternatively, when the need for two active sites is dictated by the reaction mechanism, it has been generally observed that although no synergetic effect is found in their combination, close proximity of both active sites (*e.g.* metal nanoparticles) greatly enhances the overall process yield. Accordingly, future research should promote the heterogenisation of oxidation catalysts, especially Fenton catalysts, for this specific purpose. In this task, the nature and properties of the support have demonstrated to be of paramount importance as they not only determine the particle size of nanoparticles, site dispersion and their stability *versus* leaching, but also they, in some cases, present the active site of oxidation. Accordingly, typical supports are based on TiO_2 and SiO_2 with the mesoporous TS-1 material being the one most frequently reported due to the presence of tetrahedral coordinated Ti sites. Oxides of non-noble metals have also been reported to exert a promoting effect improving the catalytic performance. Additionally, the modification of such supports *via* metal doping still needs to be fully explored to unveil its potential.

This tandem system presents a series of advantages in terms of the environmental benefits associated with the direct synthesis of hydrogen peroxide *versus* the anthraquinone route and the associated reduced costs to the reduced number of process steps and absence of hydrogen storage. However, these benefits can be masked by the overall lower productivity achieved when compared to those oxidation processes using pre-generated hydrogen peroxide. These low yields are normally related to the low concentration of hydrogen peroxide achieved *in-situ* and/or its parallel decomposition in water. In both cases, careful analysis of the process is required in order to balance the kinetics of both tandem steps. Additionally, further strategies need to be developed to enhance the

overall H_2 efficiency of the system as a key parameter determining the process economic feasibility.

More importantly, the tandem system seems to efficiently promote the *in-situ* formation of hydroperoxo species able to activate relatively inert compounds such as methane and selectively oxidise them into their oxygenated counterparts. As an exciting example, bi-metallic AuPd catalysts have recently been shown to achieve higher yields in the oxidation of methane to methanol in the one-pot system compared to the use of pre-generated hydrogen peroxide. This development has been possible thanks to the synergetic combination of the efficiency of these catalysts towards the direct synthesis of H_2O_2 from H_2 and O_2 with high selectivity and towards selective oxidation achieved by the catalytic development carried out in Hutching's group. Similar strategies and a deep understanding of the complex reaction mechanisms are needed to reveal the full potential of these tandem processes to efficiently promote the selective oxidation rather than the complete oxidation to CO_2. Enhancing the stability of these catalysts during the selective oxidation is also a critical issue for future commercial applications. Even though Ti-modified silica support is known to enhance the stability of metal nanoparticles, there is little understanding of the underlying basis of this phenomenon, demanding a more systematic study with the assistance of a model system.

Finally, considerations should be given to the safety issues associated to the flammability of the H_2/O_2 mixture in the tandem systems. Some studies have explored a series of O_2 and/or H_2 substitutes such as formic acid and hydroxylamine or the use of supercritical solvents. An even more attractive alternative is the use of membrane reactors to avoid the direct contact of oxygen and hydrogen in the gas phase while taking advantage of the atomic hydrogen diffusion mechanism to enhance the oxidant formation. Despite the potential of these systems and the improved safety, the over-oxidation control and the stability of the metallic membrane remain challenges.

Acknowledgements

References

[1] S. Dash, S. Patel, B.K. Mishra, Tetrahedron 65 (2009) 707–739.
[2] V.N. Parmon, G.I. Panov, A. Uriarte, A.S. Noskov, Catalysis Today 100 (2005) 115–131.
[3] C. Samanta, Applied Catalysis A: General 350 (2008) 133–149.
[4] http://www.dow.com/news/corporate/2010/20100622a.htm, 2013. Available from: http://www.dow.com/news/corporate/2010/20100622a.htm (09.09.13).
[5] http://www.dow.com/polyurethane/news/2012/20120104a.htm, 2013. Available from: http://www.dow.com/polyurethane/news/2012/20120104a.htm (09.09.13).
[6] J.K. Edwards, B.E.N.N. Solsona, A.F. Carley, A.A. Herzing, C.J. Kiely, G.J. Hutchings, Science 323 (2009) 1037–1041.
[7] J.M. Campos-Martin, G. Blanco-Brieva, J.L.G. Fierro, Angewandte Chemie-International Edition 45 (2006) 6962–6984.
[8] P. Landon, P.J. Collier, A.J. Papworth, C.J. Kiely, G.J. Hutchings, Chemical Communications (2002) 2058–2059.
[9] J.K. Edwards, B.E. Solsona, P. Landon, A.F. Carley, A. Herzing, C.J. Kiely, G.J. Hutchings, Journal of Catalysis 236 (2005) 69–79.
[10] M.G. Clerici, P. Ingallina, Catalysis Today 41 (1998) 351–364.
[11] T. Hayashi, K. Tanaka, M. Haruta, Journal of Catalysis 178 (1998) 566–575.
[12] R. Meiers, U. Dingerdissen, W.F. Holderich, Journal of Catalysis 176 (1998) 376–386.
[13] M. Haruta, Cattech 6 (2002) 102–115.

[14] T.A. Nijhuis, M. Makkee, J.A. Moulijn, B.M. Weckhuysen, Industrial & Engineering Chemistry Research 45 (2006) 3447–3459.
[15] B.K. Min, C.M. Friend, Chemical Reviews 107 (2007) 2709–2724.
[16] C.X. Qi, Gold Bulletin 41 (2008) 224–234.
[17] A.K. Sinha, S. Seelan, T. Akita, S. Tsubota, M. Haruta, Applied Catalysis A: General 240 (2003) 243–252.
[18] B. Chowdhury, J.J. Bravo-Suarez, N. Mimura, J.Q. Lu, K.K. Bando, S. Tsubota, M. Haruta, Journal of Physical Chemistry B 110 (2006) 22995–22999.
[19] Q.L. Chen, E.J. Beckman, Green Chemistry 10 (2008) 934–938.
[20] S. Hikazudani, T. Mochida, N. Matsuo, K. Nagaoka, T. Ishihara, H. Kobayashi, Y. Takita, Journal of Molecular Catalysis A: Chemical 358 (2012) 89–98.
[21] M. Haruta, N. Yamada, T. Kobayashi, S. Iijima, Journal of Catalysis 115 (1989) 301–309.
[22] T.A. Nijhuis, T. Visser, B.M. Weckhuysen, Journal of Physical Chemistry B 109 (2005) 19309–19319.
[23] B. Taylor, J. Lauterbach, W.N. Delgass, Applied Catalysis A: General 291 (2005) 188–198.
[24] C. Sivadinarayana, T.V. Choudhary, L.L. Daemen, J. Eckert, D.W. Goodman, Journal of the American Chemical Society 126 (2004) 38–39.
[25] A.K. Sinha, S. Seelan, S. Tsubota, M. Haruta, Topics in Catalysis 29 (2004) 95–102.
[26] J.Q. Chen, S.J.A. Halin, J.C. Schouten, T.A. Nijhuis, Faraday Discussions 152 (2011) 321–336.
[27] J.J. Bravo-Suarez, J. Lu, C.G. Dallos, T. Fujitani, S.T. Oyama, Journal of Physical Chemistry C 111 (2007) 17427–17436.
[28] A.M. Joshi, W.N. Delgass, K.T. Thomson, Journal of Physical Chemistry C 111 (2007) 7841–7844.
[29] T.A.R. Nijhuis, T. Visser, B.M. Weckhuysen, Angewandte Chemie-International Edition 44 (2005) 1115–1118.
[30] A. Ruiz, B. van der Linden, M. Makkee, G. Mul, Journal of Catalysis 266 (2009) 286–290.
[31] T.A. Nijhuis, T.Q. Gardner, B.M. Weckhuysen, Journal of Catalysis 236 (2005) 153–163.
[32] T.A. Nijhuis, B.M. Weckhuysen, Catalysis Today 117 (2006) 84–89.
[33] J.Q. Chen, S.J.A. Halin, E.A. Pidko, M. Verhoeven, D.M.P. Ferrandez, E.J.M. Hensen, J.C. Schouten, T.A. Nijhuis, Chemcatchem 5 (2013) 467–478.
[34] J.J. Bravo-Suarez, K.K. Bando, J.I. Lu, M. Haruta, T. Fujitani, S.T. Oyama, Journal of Physical Chemistry C 112 (2008) 1115–1123.
[35] T.A. Nijhuis, B.J. Huizinga, M. Makkee, J.A. Moulijn, Industrial & Engineering Chemistry Research 38 (1999) 884–891.
[36] G. Mul, A. Zwijnenburg, B. van der Linden, M. Makkee, J.A. Moulijn, Journal of Catalysis 201 (2001) 128–137.
[37] B.S. Uphade, T. Akita, T. Nakamura, M. Haruta, Journal of Catalysis 209 (2002) 331–340.
[38] E.E. Stangland, B. Taylor, R.P. Andres, W.N. Delgass, Journal of Physical Chemistry B 109 (2005) 2321–2330.
[39] C.X. Qi, T. Akita, M. Okumura, K. Kuraoka, M. Haruta, Applied Catalysis A: General 253 (2003) 75–89.
[40] C.H. Liu, Y.J. Guan, E.J.M. Hensen, J.F. Lee, C.M. Yang, Journal of Catalysis 282 (2011) 94–102.
[41] B. Chowdhury, K.K. Bando, J.J. Bravo-Suarez, S. Tsubota, M. Haruta, Journal of Molecular Catalysis A: Chemical 359 (2012) 21–27.
[42] E.E. Stangland, K.B. Stavens, R.P. Andres, W.N. Delgass, Journal of Catalysis 191 (2000) 332–347.
[43] H.W. Yang, D.L. Tang, X.N. Lu, Y.Z. Yuan, Journal of Physical Chemistry C 113 (2009) 8186–8193.
[44] Qi, C.X., T. Akita, M. Okumura, and M. Haruta, Applied Catalysis a-General. 218 (2001) 81–89.
[45] B. Chowdhury, J.J. Bravo-Suarez, M. Date, S. Tsubota, M. Haruta, Angewandte Chemie-International Edition 45 (2006) 412–415.
[46] T.A. Nijhuis, B.M. Weckhuysen, Chemical Communications (2005) 6002–6004.
[47] B.S. Uphade, Y. Yamada, T. Akita, T. Nakamura, M. Haruta, Applied Catalysis A: General 215 (2001) 137–148.
[48] L. Xu, Y.J. Ren, H.H. Wu, Y.M. Liu, Z.D. Wang, Y.T. Zhang, J.J. Xu, H.G. Peng, P. Wu, Journal of Materials Chemistry 21 (2011) 10852–10858.
[49] A.K. Sinha, S. Seelan, S. Tsubota, M. Haruta, Angewandte Chemie-International Edition 43 (2004) 1546–1548.
[50] T.A. Nijhuis, E. Sacaliuc-Parvulescu, N.S. Govender, J.C. Schouten, B.M. Weckhuysen, Journal of Catalysis 265 (2009) 161–169.
[51] E. Sacaliuc-Parvulescu, H. Friedrich, R. Palkovits, B.M. Weckhuysen, T.A. Nijhuis, Journal of Catalysis 259 (2008) 43–53.
[52] Y.A. Kalvachev, T. Hayashi, S. Tsubota, M. Haruta, Journal of Catalysis 186 (1999) 228–233.
[53] J.Q. Lu, X.M. Zhang, J.J. Bravo-Suarez, K.K. Bando, T. Fujitani, S.T. Oyama, Journal of Catalysis 250 (2007) 350–359.
[54] E. Sacaliuc, A.M. Beale, B.M. Weckhuysen, T.A. Nijhuis, Journal of Catalysis 248 (2007) 235–248.
[55] L. Cumaranatunge, W.N. Delgass, Journal of Catalysis 232 (2005) 38–42.
[56] W.S. Lee, M.C. Akatay, E.A. Stach, F.H. Ribeiro, W.N. Delgass, Journal of Catalysis 287 (2012) 178–189.
[57] A.K. Sinha, S. Seelan, T. Akita, S. Tsubota, M. Haruta, Catalysis Letters 85 (2003) 223–228.
[58] G.W. Zhan, M.M. Du, J.L. Huang, Q.B. Li, Catalysis Communications 12 (2011) 830–833.

[59] G.W. Zhan, M.M. Du, D.H. Sun, J.L. Huang, X. Yang, Y. Ma, A.R. Ibrahim, Q.B. Li, Industrial & Engineering Chemistry Research 50 (2011) 9019–9026.
[60] F.S. Wang, C.X. Qi, J.T. Ma, Catalysis Communications 8 (2007) 1947–1952.
[61] B. Taylor, J. Lauterbach, W.N. Delgass, Catalysis Today 123 (2007) 50–58.
[62] J.Q. Lu, X.M. Zhang, J.J. Bravo-Suarez, T. Fujitani, S.T. Oyama, Catalysis Today 147 (2009) 186–195.
[63] C.X. Qi, J.H. Huang, S.Q. Bao, H.J. Su, T. Akita, M. Haruta, Journal of Catalysis 281 (2011) 12–20.
[64] Mennemann, C. and P. Claus, Catalysis Letters. 134 (2010) 31-36.
[65] T. Liu, P. Hacarlioglu, S.T. Oyama, M.F. Luo, X.R. Pan, J.Q. Lu, Journal of Catalysis 267 (2009) 202–206.
[66] R. Meiers, W.F. Holderich, Catalysis Letters 59 (1999) 161–163.
[67] R.P. Wang, X.W. Guo, X.S. Wang, J.Q. Hao, Catalysis Letters 90 (2003) 57–63.
[68] R.P. Wang, X.W. Guo, X.S. Wang, J.Q. Hao, Catalysis Today 93–95 (2004) 217–222.
[69] R.P. Wang, X.W. Guo, X.S. Wang, J.Q. Hao, G. Li, J.H. Xiu, Applied Catalysis A: General 261 (2004) 7–13.
[70] J.H. Huang, M. Haruta, Research on Chemical Intermediates 38 (2012) 1–24.
[71] W. Laufer, W.F. Hoelderich, Applied Catalysis A: General 213 (2001) 163–171.
[72] G. Jenzer, T. Mallat, M. Maciejewski, F. Eigenmann, A. Baiker, Applied Catalysis A: General 208 (2001) 125–133.
[73] J.E. Remias, A. Sen, Journal of Molecular Catalysis A: Chemical 189 (2002) 33–38.
[74] E.J. Beckman, Green Chemistry 5 (2003) 332–336.
[75] C.F. Shi, B. Zhu, M. Lin, J. Long, Catalysis Letters 133 (2009) 70–75.
[76] S. Hikazudani, T. Mochida, K. Yano, K. Nagaoka, T. Ishihara, Y. Takita, Catalysis Communications 12 (2011) 1396–1400.
[77] Q. Jin, J. Bao, H. Sakiyama, N. Tsubaki, Research on Chemical Intermediates 37 (2011) 177–184.
[78] P.P. Notte, Topics in Catalysis 13 (2000) 387–394.
[79] J.E. Remias, T.A. Pavlosky, A. Sen, Journal of Molecular Catalysis A: Chemical 203 (2003) 179–192.
[80] A. Kunai, T. Kitano, Y. Kuroda, J. Lifen, K. Sasaki, Catalysis Letters 4 (1990) 139–144.
[81] T. Miyake, M. Hamada, Y. Sasaki, M. Oguri, Applied Catalysis A: General 131 (1995) 33–42.
[82] T. Kitano, T. Wani, T. Ohnishi, J. Lifen, Y. Kuroda, A. Kunai, K. Sasaki, Catalysis Letters 11 (1991) 11–18.
[83] T. Kitano, Y. Kuroda, M. Mori, S. Ito, K. Sasaki, M. Nitta, Journal of the Chemical Society-Perkin Transactions 2 (1993) 981–985.
[84] H. Ehrich, H. Berndt, M.M. Pohl, K. Jahnisch, M. Baerns, Applied Catalysis A: General 230 (2002) 271–280.
[85] T. Tatsumi, K. Yuasa, H. Tominaga, Journal of the Chemical Society-Chemical Communications (1992) 1446–1447.
[86] X.B. Wang, X.F. Zhang, H.O. Liu, J.S. Qiu, W. Han, K.L. Yeung, Catalysis Today 193 (2012) 151–157.
[87] W. Laufer, J.P.M. Niederer, W.F. Hoelderich, Advanced Synthesis & Catalysis 344 (2002) 1084–1089.
[88] W. Laufer, W.F. Hoelderich, Chemical Communications (2002) 1684–1685.
[89] S. Niwa, M. Eswaramoorthy, J. Nair, A. Raj, N. Itoh, H. Shoji, T. Namba, F. Mizukami, Science 295 (2002) 105–107.
[90] N. Itoh, S. Niwa, F. Mizukami, T. Inoue, A. Igarashi, T. Namba, Catalysis Communications 4 (2003) 243–246.
[91] G.D. Vulpescu, M. Ruitenbeek, L.L. van Lieshout, L.A. Correia, D. Meyer, P. Pex, Catalysis Communications 5 (2004) 347–351.
[92] K. Sato, T.A. Hanaoka, S. Niwa, C. Stefan, T. Namba, F. Mizukami, Catalysis Today 104 (2005) 260–266.
[93] S.L. Shu, Y. Huang, X.J. Hu, Y.Q. Fan, N.P. Xu, Journal of Physical Chemistry C 113 (2009) 19618–19622.
[94] S.Y. Ye, S. Hamakawa, S. Tanaka, K. Sato, M. Esashi, F. Mizukami, Chemical Engineering Journal 155 (2009) 829–837.
[95] L. Bortolotto, R. Dittmeyer, Separation and Purification Technology 73 (2010) 51–58.
[96] Y. Guo, X.B. Wang, X.F. Zhang, Y. Wang, H.O. Liu, J.Q. Wang, J.S. Qiu, K.L. Yeung, Catalysis Today 156 (2010) 282–287.
[97] R. Dittmeyer, L. Bortolotto, Applied Catalysis A: General 391 (2011) 311–318.
[98] X.B. Wang, Y. Guo, X.F. Zhang, Y. Wang, H.O. Liu, J.Q. Wang, J.S. Qiu, K.L. Yeung, Catalysis Today 156 (2010) 288–294.
[99] C. Basheer, Journal of Chemistry 2013 (2013) 1–10.
[100] F.R. Garcia-Garcia, L. Torrente-Murciano, D. Chadwick, K. Li, Journal of Membrane Science 405 (2012) 30–37.
[101] R.A. Periana, D.J. Taube, S. Gamble, H. Taube, T. Satoh, H. Fujii, Science 280 (1998) 560–564.
[102] R. Palkovits, M. Antonietti, P. Kuhn, A. Thomas, F. Schuth, Angewandte Chemie-International Edition 48 (2009) 6909–6912.
[103] C. Hammond, M.M. Forde, M.H. Ab Rahim, A. Thetford, Q. He, R.L. Jenkins, N. Dimitratos, J.A. Lopez-Sanchez, N.F. Dummer, D.M. Murphy, A.F. Carley, S.H. Taylor, D.J. Willock, E.E. Stangland, J. Kang, H. Hagen, C.J. Kiely, G.J. Hutchings, Angewandte Chemie-International Edition 51 (2012) 5129–5133.
[104] M.R. Lin, T. Hogan, A. Sen, Journal of the American Chemical Society 119 (1997) 6048–6053.
[105] C.Y. Shen, E.A. Garcia-Zayas, A. Sen, Journal of the American Chemical Society 122 (2000) 4029–4031.
[106] E.D. Park, S.H. Choi, J.S. Lee, Journal of Catalysis 194 (2000) 33–44.
[107] J.S. Min, H. Ishige, M. Misono, N. Mizuno, Journal of Catalysis 198 (2001) 116–121.
[108] E.D. Park, Y.S. Hwang, J.S. Lee, Catalysis Communications 2 (2001) 187–190.
[109] E.D. Park, Y.S. Hwang, C.W. Lee, J.S. Lee, Applied Catalysis A: General. 247 (2003) 269–281.
[110] Y.F. Fan, Z.J. An, X.L. Pan, X.M. Liu, X.H. Bao, Chemical Communications (2009) 7488–7490.
[111] M.R. Lin, T.E. Hogan, A. Sen, Journal of the American Chemical Society 118 (1996) 4574–4580.
[112] M.H. Ab Rahim, M.M. Forde, R.L. Jenkins, C. Hammond, Q. He, N. Dimitratos, J.A. Lopez-Sanchez, A.F. Carley, S.H. Taylor, D.J. Willock, D.M. Murphy, C.J. Kiely, G.J. Hutchings, Angewandte Chemie-International Edition 52 (2013) 1280–1284.
[113] J.J. Bravo-Suarez, K.K. Bando, T. Fujitani, S.T. Oyama, Journal of Catalysis 257 (2008) 32–42.
[114] M.S. Yalfani, S. Contreras, F. Medina, J.E. Sueiras, Journal of Hazardous Materials 192 (2011) 340–346.
[115] M.S. Yalfani, S. Contreras, J. Llorca, M. Dominguez, J.E. Sueiras, F. Medina, Physical Chemistry Chemical Physics 12 (2010) 14673–14676.
[116] M.S. Yalfani, S. Contreras, F. Medina, J. Sueiras, Applied Catalysis B: Environmental 89 (2009) 519–526.
[117] S.Y. Yuan, Y. Fan, Y.C. Zhang, M. Tong, P. Liao, Environmental Science & Technology 45 (2011) 8514–8520.
[118] A. Turki, H. Kochkar, G. Berhault, A. Ghorbel, p-Hydroxybenzoic acid degradation by Fe/Pd-HNT catalysts with in situ generated hydrogen peroxide, in: E.M. Gaigneaux, et al. (Eds.) Scientific Bases for the Preparation of Heterogeneous Catalysts: Proceedings of the 10th International Symposium, 2010, Elsevier Science BV, Amsterdam, pp. 593–596.
[119] O. Osegueda, A. Dafinov, J. Llorca, F. Medina, J. Suerias, Catalysis Today 193 (2012) 128–136.
[120] L.Y. Kong, G. Li, X.S. Wang, Catalysis Letters 92 (2004) 163–167.
[121] L.Y. Kong, G. Li, X.S. Wang, Catalysis Today 93–95 (2004) 341–345.
[122] S.Q. Ma, G. Li, X.S. Wang, Chemical Engineering Journal 156 (2010) 532–539.
[123] C.F. Shi, B. Zhu, M. Lin, J. Long, Catalysis Today 149 (2010) 132–137.
[124] H.Y. Song, G. Li, X.S. Wang, Y.Y. Chen, Microporous and Mesoporous Materials 139 (2011) 104–109.
[125] S.K. Karmee, L. Greiner, A. Kraynov, T.E. Muller, B. Niemeijer, W. Leitner, Chemical Communications 46 (2010) 6705–6707.
[126] K. Sato, M. Hyodo, M. Aoki, X.Q. Zheng, R. Noyori, Tetrahedron 57 (2001) 2469–2476.
[127] W.S. Lee, L.C. Lai, M.C. Akatay, E.A. Stach, F.H. Ribeiro, W.N. Delgass, Journal of Catalysis 296 (2012) 31–42.
[128] M.S. Yalfani, A. Georgi, S. Contreras, F. Medina, F.D. Kopinke, Applied Catalysis B: Environmental 104 (2011) 161–168.